Princeton Plasma Physics Laboratory

PPPL- 4714

PPPL- 4714

Mirror Force Induced Wave Dispersion in Alfven Waves

P.A. Damiano and J.R. Johnson

November, 2011

Prepared for the U.S. Department of Energy under Contract DE-AC02-09CH11466.

Mirror force induced wave dispersion in Alfvén waves

P.A. Damiano and J.R. Johnson

Princeton Plasma Physics Laboratory, Princeton, New Jersey

(Dated: November 23, 2011)

Abstract

A recent series of studies of the upward current region of global scale Field Line Resonances using a hybrid MHD-kinetic electron model shows that the parallel current profile saturates and broadens perpendicular to the ambient magnetic field and that the extent of this broadening increases with the electron temperature. Using MHD simulations, with a parallel Ohm's law derived from the hybrid simulation results at different temperatures, we explore the nature of this broadening and illustrate that this dispersion is a result of the increased perpendicular Poynting flux resulting from the increased parallel electric field associated with mirror force effects. The increased perpendicular Poynting flux facilitates a dispersion of wave energy across magnetic field lines which in-turn allows for the acceleration of electrons to carry the field aligned current on adjacent field lines. This dispersion is additionally amplified as a function of time in the simulation as the precipitation of weakly trapped electrons requires a progressively larger parallel electric field to accelerate more strongly trapped populations to carry the current.

Preprint submitted to Physical Review Letters

INTRODUCTION

Field Line Resonances (FLRs) are ultra low frequency (mHz) standing shear Alfvén waves structures that form along the Earth's closed dipolar magnetic field lines and have been linked to the formation of some discrete auroral arcs (e.g. Refs. [1–3]). In order to understand how electrons are accelerated to sufficient energies within these waves to drive auroral emissions, a number of studies, including both theoretical [4, 5] and simulations ([6–8]), have looked to mirror force effects as a candidate to account for the keV potential drops needed to accelerate electrons to sufficient energies to explain the auroral emissions. Refs. [7, 8] considered the upward current region (corresponding to the downward propagation of magnetospheric electrons) of a toroidal FLR system using a 2-D hybrid MHD-kinetic electron model in dipolar coordinates for a constant resonance width and a range of electron thermal temperatures from 5 eV to a keV. A saturation and broadening of parallel current profile perpendicular to the magnetic field was noted that was enhanced by a depletion of electrons at small pitch angles. The magnitude of the broadening was found to increase substantially with the temperature of the electron distribution function. Fundamentally, a perpendicular dispersion of wave energy should result when there is a cross field component to the Poynting flux, which occurs when there is a parallel component of the electric field. This dispersion is well known in the context of electron inertial or kinetic Alfvén waves, but has not been addressed in the context of a mirror kinetic Alfvén wave (to borrow the terminology of Ref. [5]). In order to understand if mirror force effects on the parallel electric field can account for the broadening evident in these aforementioned kinetic simulations, in the present study we consider a simplified MHD description that incorporates the idea that the parallel electric field increases with temperature (to overcome the resistance of the mirror force) via a simple Ohm's law description ($j_{||} = \sigma_{||} E_{||}$) where the temperature effects on $E_{||}$ are incorporated into our assumption for the parallel conductivity $\sigma_{||}$. This simplified analysis allows us to separate out the effects of the complicated wave particle interactions evident in the hybrid simulations and focus on the effects of $E_{||}$ alone.

The rest of the paper is broken up into four sections. Section 2 summarizes the hybrid and MHD models. Section 3 presents our simulation results while Section 4 gives our conclusions.

HYBRID AND MHD MODELS

Two models will be utilized in the present study. The first is the hybrid MHD kinetic-electron model presented initially in Ref. [6] and used in Refs. [7, 8]. The model geometry is presented in Figure 1 where x_1 is the field aligned direction and x_2 is the direction across L shells. The model couples the azimuthal components of the linearized cold plasma MHD momentum equation (u_3) and Faraday's law (b_3) given respectively by

$$\mu_o \rho_o \frac{\partial u_3}{\partial t} = \frac{B_o}{h_1 h_3}\left(\frac{\partial}{\partial x_1}(h_3 b_3)\right) \tag{1}$$

$$\frac{\partial b_3}{\partial t} = \frac{-1}{h_1 h_2}\left(\frac{\partial}{\partial x_1}(h_2 E_2) - \frac{\partial}{\partial x_2}(h_1 E_1)\right) \tag{2}$$

with the perpendicular Ohm's law

$$E_2 = -u_3 B_o \tag{3}$$

and the guiding center equations for electron dynamics

$$m_e \frac{dv_1}{dt} = -eE_1 - \mu_m \frac{1}{h_1}\frac{\partial B_o}{\partial x_1} \tag{4}$$

$$h_1 \frac{dx_1}{dt} = v_1 \tag{5}$$

where v_1 is the parallel electron velocity, $x_1 = \cos\theta/r^2$, $x_2 = \sin^2\theta/r$, $x_3 = \phi$, $h_1 = r^3/(1+3\cos^2\theta)^{1/2}$, $h_2 = r^2/(\sin\theta(1+3\cos^2\theta)^{1/2})$, $h_3 = r\sin\theta$ and $\mu_m = m_e v_\perp^2/(2B)$ is the magnetic moment. Equations (1) - (3) with $E_1 = 0$, provides a self-consistent linear model of Alfvén wave propagation where massless electrons respond to ion polarization currents perpendicular to the ambient magnetic field in order to maintain quasineutrality. The MHD and kinetic portions of the model are closed via the algorithm for the parallel electric field which incorporates the generalized Ohm's law (including electron inertia, electron pressure and mirror force contributions) and an auxilliary Poisson's equations for the enforcement of quasineutrality [6].

The results of the kinetic model are compared with an MHD description incorporating equations (1) - (3) along with a simple parallel Ohm's law given by $E_{||} = E_1 = (1/\sigma_1)j_1$ where we will consider the current saturation and broadening in the ideal case ($\sigma_1 = 0$) and

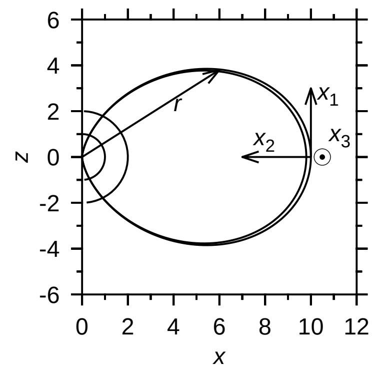

FIG. 1. Simulation domain where x_3 is positive increasing out of the page. The circles of radius 1 and 2 R_E respectively denote the surface of the Earth and "ionospheric" boundary. The angle θ is subtended from the z axis. Perpendicular boundaries are at L=9.4 and L=10. (From Ref. [7]).

for cases where constant values of σ_1 are chosen based on the ratio of E_1/j_1 approximately consistent with the hybrid MHD-kinetic simulations at different temperatures.

SIMULATIONS

In order to interpret the current broadening seen in Refs. [7, 8], the simulations are initialized in the same manner by perturbing the azimuthal fluid velocity in Equation (1) using an approximate fundamental mode eignemode solution of a standing mode along an L=10 magnetic field line [6] based on the analytical model of Ref. [9]. Perpendicular to the magnetic field, the initial perturbation has a 1/2 Gaussian profile that allows for the consideration of only an upward current region corresponding to the downward acceleration of magnetospheric electrons. The Full Width Half Maximum of the perpendicular Gaussian profile at the equator was 0.5 R_E.

Figure 2 displays the hybrid model parallel current density, j_1, at the northern ionospheric boundary for electron temperatures of 200 eV (Figure 2a) and a keV (Figure 2b) at two different times. Superimposed on the hybrid model results is the corresponding MHD solution with $E_1 = 0$ (no resistivity) at the later time ($t = 0.2\ T_A$). The parallel current, j_1 grows with time but then eventually saturates and broadens relative to the ideal MHD solution with the extent of the broadening proportional to the temperature. The saturation and broadening was also noted in Refs. [7, 8] using the same simulation code.

The middle panels of Figure 2 display the distribution function (at the position of the

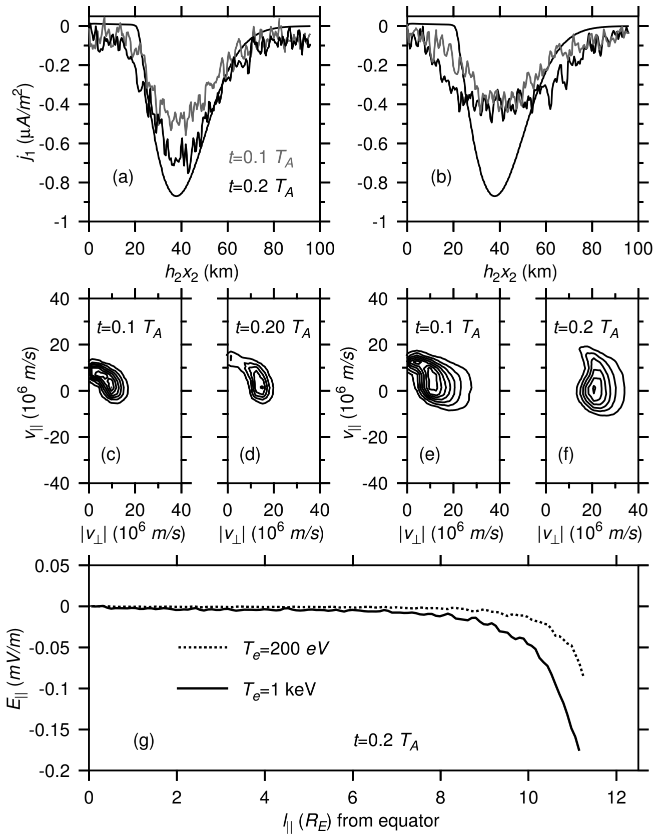

FIG. 2. The hybrid model parallel current j_1 as a function of perpendicular distance across the simulation domain (h_2x_2) at the northern ionospheric boundary for (a) $T_e = 200\ eV$ and (b) $T_e =$ keV. Smooth black lines show the MHD result. (c)+(d) Distribution function evolution at current maximum ($h_2x_2 = 38$ km) for $T_e = 200\ eV$. (e)+(f) Distribution function evolution at current maximum for $T_e = 1$ keV. (g) Parallel electric field along the field line from the equator to the northern ionospheric boundary at the position of the current maximum ($h_2x_2 = 38$ km).

current maximum) for the same times as the plots in Figures 2a and 2b. The effect of the mirror force on the electron dynamics is clear from the ring distributions which result as some of electrons, accelerated to carry the field aligned current, undergo mirroring and travel back up the field line. The radius of the ring is larger in the $T_e = 1$ keV case since as temperature increases, a larger fraction of electrons will experience a mirror force sufficiently strong to overcome the accelerating potential and be reflected back up the field line. The remaining downward propagating population must therefore be accelerated more to carry the field aligned current. The gradual depletion of electrons at small pitch angles (particularly in the $T_e = 1$ keV case) coincides with a further broadening of the parallel current profile

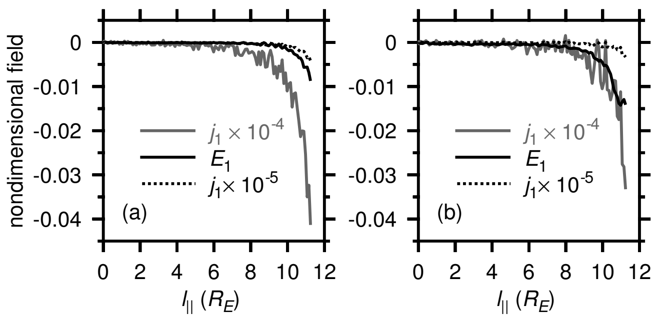

FIG. 3. Hybrid model parallel electric field (along field line of maximum j_1) as a function of distance along the field line, $l_{||}$ (measured from equator) at t=0.15 T_A, along with the corresponding profile for j_1 multiplied by 10^{-5} (dotted line) and 10^{-4} (gray line). (a) $T_e = 200$ eV. (b) $T_e = 1$ keV.

from $t = 0.1\ T_A$ to $t = 0.2\ T_A$

The need to accelerate fewer untrapped electrons in the keV case to carry the current, requires a correspondingly larger parallel electric field than the 200 eV case as illustrated in Figure 2f, which plots the parallel electric field along the field line at the position of the current maximum ($h_2 x_2 = 38$ km in Figure 2a). Although the current is reduced in the keV case, the mirror force effects still result in a significantly larger parallel electric field (relative to the 200 eV case), which is capable of accelerating electrons to observed keV energies ([8]).

The dispersion of wave energy across magnetic field lines has long been associated with electron inertial and kinetic Alfvén wave limits where the presence of E_1 implies perpendicular Poynting flux ($S_2 = -E_1 b_3$), which propagates wave energy across magnetic field lines. However, in a system dominated by mirror force effects, the driving force for generating E_1 is different, but the net effect is the same. In order to separate whether the dispersion seen in the hybrid simulations is simply associated with the magnitude of this E_1 and not with any other wave-particle interaction, we revisit the broadening evident in Figure 2 with the MHD model discussed in the last section. In order to choose values for σ_1 in the expression for E_1 we appeal to the hybrid simulations for a time consistent with the interval in Figure 2. Figure 3 displays the field-aligned profiles of E_1 and $j_1(1/\sigma_1)$ in the middle of the time interval (t=0.15 T_A) for the temperature cases considered in Figure 2. Ratios of $1/\sigma_1 \sim 10^{-5}$ qualitatively represents the $T_e = 200\ eV$ case while, $1/\sigma_1 \sim 10^{-4}$ is more appropriate for the keV case. With the depletion of electrons at small pitch angles evident in the middle panels of Figure 2, E_1 increases to accelerate more strongly trapped particles, while the parallel current saturates causing the E_1/j_1 ratio to increase with time. The change is slow however, and we therefore conducted simulations with the MHD model using the relevant bounding limits ($1/\sigma_1 = 10^{-4}$ and $1/\sigma_1 = 10^{-5}$) for the time frame from t=0.1 to 0.2 T_A . The resulting ionospheric parallel current profiles are plotted in Figure 4 along with the hybrid solutions at the same time and the qualitative features of the broadening are reproduced remarkably well by this simple assumption in contrast with the ideal MHD results shown in Figure 2. Additional broadening can occur with time as E_1 increases (up to 1/4 period) to accelerate more strongly trapped electrons in order to carry the saturated current. The drop in total current evident from the $T_e = 200$ keV to the $T_e = 1$ keV case occurs because more wave energy is lost to the increased electron energization in the latter case (refer to Figure 2 and Ref. [7]). In the MHD equivalent, the energy is lost to j_1E_1 Ohmic dissipation, but as expected by the results of Figure 4, the characteristics of the dissipation follow closely the hybrid $T_e = 1$ keV case (Figure 5b).

Consistent with previous comments, a plot of the perpendicular Poynting flux (Figure 5) in the $1/\sigma_1 = 10^{-4}$ case is substantially increased in magnitude and of wider perpendicular extent than the $1/\sigma_1 = 10^{-5}$ case, confirming the simple, yet profound, interpretation that the E_1 associated with mirror force effects leads to the wave dispersion evident in the hybrid simulations. This dispersion in-turn limits the current growth in the original profile leading to the noted saturation. The peak in S_2 is slightly offset to the left from the peak in j_1 (Figure 4) as b_3 has a tanh profile which is maximum to the left and in-turn promotes slightly more wave dispersion in this direction.

The dispersion of wave energy across magnetic field lines in the context of electron inertial or kinetic Alfven waves has been understood for a long time. However, we do not believe that it has been widely recognized that dispersion in itself is dependent only on the presence of a parallel electric field, while the nature of the source of $E_{||}$ will define the details and extent of that dispersion. By contrasting the hybrid and MHD simulations in this simple study we have illustrated that the mirror force in a mirror kinetic Alfvén wave can lead to significant dispersion of wave energy in the upward current region of large scale waves.

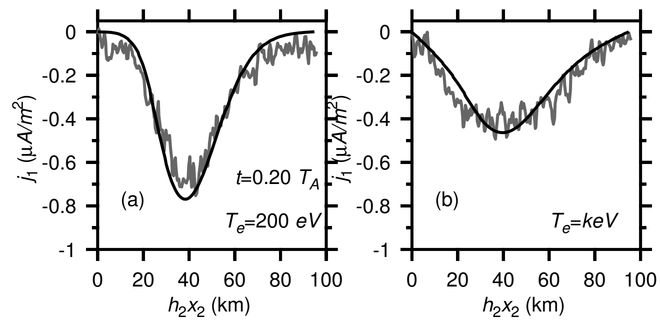

FIG. 4. Contrasting parallel current profile at northern ionospheric boundary between the MHD (black lines) and hybrid (gray lines) models for (a) $1/\sigma_1 = 10^{-5}$ and $T_e = 200\ eV$ and (b) $1/\sigma_1 = 10^{-4}$ and $T_e = 1$ keV.

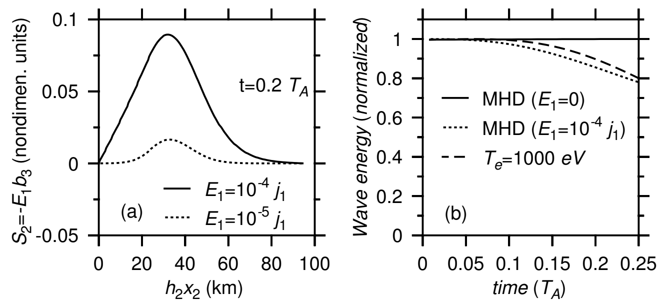

FIG. 5. a) Perpendicular Poynting flux, $S_2 = -E_1 b_3$ from the MHD model at the northern ionospheric boundary. b) Time evolution of the total wave energy (sum of ion kinetic and magnetic energies) for the MHD model with $E_1 = 0$ and $E_1 = 10^{-4} j_1$ and the hybrid model for $T_e = 1$ keV.

CONCLUSIONS

Using a simplified MHD description, we have explained a perpendicular broadening of the parallel current profile that has appeared in hybrid MHD-kinetic electron simulations of the upward current region of geomagnetic Field Line Resonances. The broadening increases with temperature in the hybrid system because mirror force effects ($\mu\nabla B$) dominate the parallel electric field generation. The same saturation and broadening of the field aligned current was also seen in resistive MHD simulations where the parallel Ohm's law was specified based on the kinetic-MHD simulations for a range of temperatures. This simplified description allows consideration of the broadening in the absence of other wave-particle interactions evident in the kinetic simulations. Therefore, the fact that the MHD results reproduce remarkably well the broadening evident in the hybrid model results confirms that $E_{||}$ associated with mirror force effects is driving the perpendicular dispersion. The increased $E_{||}$ facilitates increased perpendicular Poynting flux which in-turn propagates wave energy across magnetic field lines. Although we have applied this analysis to a Field Line Resonance system, the low frequency nature of these waves implies that the results are also applicable to auroral arc structures that result from quasi-static potential drops. Additionally, although, mirror force effects dominate the parallel electric field generation within the hybrid model, the MHD analysis is completely general and so any source of $E_{||}$ of consistent magnitude would lead to similar dispersion. Future work would be to quantify systematically the dependence of $\sigma_{||}$ on temperature, possibly by means of the derivation of a non-local conductivity tensor that incorporates the effects of mirror force trapping (e.g. Refs. [4, 10]).

The authors acknowledge support from NASA grants (NNG07EK69I, NNH07AF37I, NNH09AM53I, and NNH09AK63I), NSF grant ATM0902730, and DOE contract DE-AC02-09CH11466.

[1] B. L. Xu, J. C. Samson, W. W. Liu, F. Creutzberg, and T. J. Hughes, J. Geophys. Res., **98**, 11531 (1993).

[2] W. Lotko, A. V. Streltsov, and C. W. Carlson, Geophys. Res. Lett., **25**, 4449 (1998).

[3] J. C. Samson, R. Rankin, and V. T. Tikhonchuk, Ann. Geophys., **21**, 933 (2003).

[4] R. Rankin, J. C. Samson, and V. T. Tikhonchuk, Geophys. Res. Lett., **26**, 3601 (1999).

[5] T. K. Nakamura, J. Geophys. Res., **105**, 10729 (2000).

[6] P. A. Damiano, A. N. Wright, R. D. Sydora, and J. C. Samson, Phys. Plasmas, **14**, 062904 (2007).

[7] P. A. Damiano and A. N. Wright, J. Geophys. Res., **113**, A09219 (2008).

[8] P. A. Damiano and J. R. Johnson, submitted to Geophys. Res. Lett. (2011).

[9] J. P. H. Taylor and A. D. M. Walker, Planet. Space Sci., **32**, 1119 (1984).

[10] R. L. Lysak and Y. Song, J. of Geophys. Res., **108**, 1327 (2003).

The Princeton Plasma Physics Laboratory is operated
by Princeton University under contract
with the U.S. Department of Energy.

Information Services
Princeton Plasma Physics Laboratory
P.O. Box 451
Princeton, NJ 08543

Phone: 609-243-2245
Fax: 609-243-2751
e-mail: pppl_info@pppl.gov
Internet Address: http://www.pppl.gov